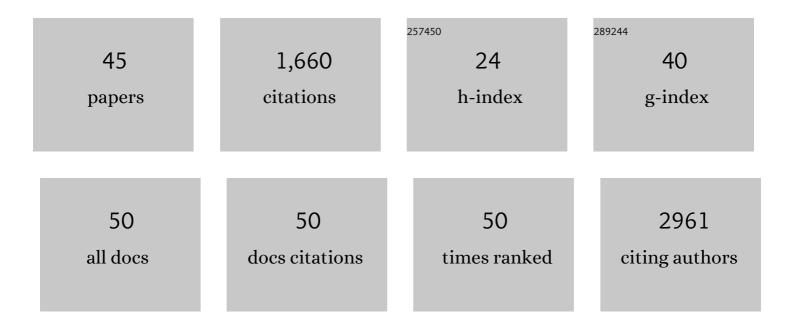
Guadalupe Soria

List of Publications by Year in descending order

Source: https://exaly.com/author-pdf/6388232/publications.pdf Version: 2024-02-01



#	Article	IF	CITATIONS
1	Lack of CB1 Cannabinoid Receptor Impairs Cocaine Self-Administration. Neuropsychopharmacology, 2005, 30, 1670-1680.	5.4	197
2	Acute Damage to the Posterior Limb of the Internal Capsule on Diffusion Tensor Tractography as an Early Imaging Predictor of Motor Outcome after Stroke. American Journal of Neuroradiology, 2011, 32, 857-863.	2.4	151
3	Quantification of Thrombus Hounsfield Units on Noncontrast CT Predicts Stroke Subtype and Early Recanalization after Intravenous Recombinant Tissue Plasminogen Activator. American Journal of Neuroradiology, 2012, 33, 90-96.	2.4	120
4	The Lack of A2A Adenosine Receptors Diminishes the Reinforcing Efficacy of Cocaine. Neuropsychopharmacology, 2006, 31, 978-987.	5.4	79
5	Adenosine A2A receptors are involved in physical dependence and place conditioning induced by THC. European Journal of Neuroscience, 2004, 20, 2203-2213.	2.6	74
6	Quantitative discrimination between endogenous SHG sources in mammalian tissue, based on their polarization response. Optics Express, 2009, 17, 10168.	3.4	58
7	The natural hallucinogen 5-MeO-DMT, component of Ayahuasca, disrupts cortical function in rats: reversal by antipsychotic drugs. International Journal of Neuropsychopharmacology, 2014, 17, 1269-1282.	2.1	57
8	Early brain connectivity alterations and cognitive impairment in a rat model of Alzheimer's disease. Alzheimer's Research and Therapy, 2018, 10, 16.	6.2	57
9	A reliable method to study cue-, priming-, and stress-induced reinstatement of cocaine self-administration in mice. Psychopharmacology, 2008, 199, 593-603.	3.1	52
10	Estimation of the effective orientation of the SHG source in primary cortical neurons. Optics Express, 2009, 17, 14418.	3.4	52
11	Attenuation of nicotine-induced rewarding effects in A2A knockout mice. Neuropharmacology, 2006, 51, 631-640.	4.1	50
12	A reliable model of intravenous MDMA self-administration in naÃ⁻ve mice. Psychopharmacology, 2006, 184, 212-220.	3.1	49
13	In vivo magnetic resonance imaging characterization of bilateral structural changes in experimental Parkinson's disease: a T2 relaxometry study combined with longitudinal diffusion tensor imaging and manganese-enhanced magnetic resonance imaging in the 6 European Journal of Neuroscience, 2011, 33, 1551-1560.	2.6	48
14	Increased nitric oxide production in lymphatic endothelial cells causes impairment of lymphatic drainage in cirrhotic rats. Gut, 2013, 62, 138-145.	12.1	47
15	The Ins and Outs of the BCCAo Model for Chronic Hypoperfusion: A Multimodal and Longitudinal MRI Approach. PLoS ONE, 2013, 8, e74631.	2.5	45
16	Strain-specific spleen remodelling in Plasmodium yoelii infections in Balb/c mice facilitates adherence and spleen macrophage-clearance escape. Cellular Microbiology, 2011, 13, 109-122.	2.1	43
17	Improved Assessment of <i>Ex Vivo</i> Brainstem Neuroanatomy With Highâ€Resolution MRI and DTI at 7 Tesla. Anatomical Record, 2011, 294, 1035-1044.	1.4	36
18	Structural and functional brain alterations in a murine model of Angiotensin <scp>II</scp> â€induced hypertension. Journal of Neurochemistry, 2017, 140, 509-521.	3.9	36

GUADALUPE SORIA

#	Article	IF	CITATIONS
19	The Use of a Three-Dimensional Novel Computer-Based Model for Analysis of the Endonasal Endoscopic Approach to the Midline Skull Base. World Neurosurgery, 2011, 75, 106-113.	1.3	33
20	Anatomic Skull Base Education Using Advanced Neuroimaging Techniques. World Neurosurgery, 2013, 79, S16.e9-S16.e13.	1.3	32
21	Functional anatomy of subcortical circuits issuing from or integrating at the human brainstem. Clinical Neurophysiology, 2012, 123, 4-12.	1.5	30
22	A Magnetic Resonance Image Based Atlas of the Rabbit Brain for Automatic Parcellation. PLoS ONE, 2013, 8, e67418.	2.5	30
23	A complementary diffusion tensor imaging (DTI)-histological study in a model of Huntington's disease. Neurobiology of Aging, 2012, 33, 945-959.	3.1	29
24	Reproducible imaging of rat corticothalamic pathway by longitudinal manganese-enhanced MRI (L-MEMRI). NeuroImage, 2008, 41, 668-674.	4.2	25
25	Bicosomes: Bicelles in Dilute Systems. Biophysical Journal, 2010, 99, 480-488.	0.5	25
26	M2 cortex-dorsolateral striatum stimulation reverses motor symptoms and synaptic deficits in Huntington's disease. ELife, 2020, 9, .	6.0	25
27	DWI and complex brain network analysis predicts vascular cognitive impairment in spontaneous hypertensive rats undergoing executive function tests. Frontiers in Aging Neuroscience, 2014, 6, 167.	3.4	24
28	Behavioural and biochemical responses to morphine associated with its motivational properties are altered in adenosine A _{2A} receptor knockout mice. British Journal of Pharmacology, 2008, 155, 757-766.	5.4	22
29	Regulation of the immediate-early genes arc and zif268 in a mouse operant model of cocaine seeking reinstatement. Journal of Neural Transmission, 2011, 118, 877-887.	2.8	19
30	Resting State Networks in the TgF344-AD Rat Model of Alzheimer's Disease Are Altered From Early Stages. Frontiers in Aging Neuroscience, 2019, 11, 213.	3.4	16
31	Anatomic Study of the Central Core of the Cerebrum Correlating 7-T Magnetic Resonance Imaging and Fiber Dissection With the Aid of a Neuronavigation System. Operative Neurosurgery, 2014, 10, 294-304.	0.8	13
32	Food craving-like episodes during pregnancy are mediated by accumbal dopaminergic circuits. Nature Metabolism, 2022, 4, 424-434.	11.9	13
33	Brain connectivity during Alzheimer's disease progression and its cognitive impact in a transgenic rat model. Network Neuroscience, 2020, 4, 397-415.	2.6	12
34	Increased Corticospinal Tract Fractional Anisotropy Can Discriminate Stroke Onset Within the First 4.5 Hours. Stroke, 2013, 44, 1162-1165.	2.0	11
35	Imaging white-matter pathways of the auditory system with diffusion imaging tractography. Handbook of Clinical Neurology / Edited By P J Vinken and G W Bruyn, 2015, 129, 277-288.	1.8	11
36	Endoscopic Endonasal Transclival Approach to the Ventral Brainstem: Anatomic Study of the Safe Entry Zones Combining Fiber Dissection Technique with 7 Tesla Magnetic Resonance Guided Neuronavigation. Operative Neurosurgery, 2019, 16, 239-249.	0.8	10

GUADALUPE SORIA

#	Article	IF	CITATIONS
37	Anti-Obesity Sodium Tungstate Treatment Triggers Axonal and Glial Plasticity in Hypothalamic Feeding Centers. PLoS ONE, 2012, 7, e39087.	2.5	8
38	Infarct volume prediction using apparent diffusion coefficient maps during middle cerebral artery occlusion and soon after reperfusion in the rat. Brain Research, 2014, 1583, 169-178.	2.2	6
39	Effects of Orientation and Anisometry of Magnetic Resonance Imaging Acquisitions on Diffusion Tensor Imaging and Structural Connectomes. PLoS ONE, 2017, 12, e0170703.	2.5	6
40	Polarization second harmonic generation (PSHG) imaging of neurons: estimating the effective orientation of the SHG source in axons. Proceedings of SPIE, 2010, , .	0.8	1
41	Clinical Neuropathology image 4-2017: High-resolution 7 Tesla MRI of postmortem brain specimens: improving neuroimaging-neuropathology correlations. , 2017, 36, 162-163.		1
42	Contrast enhancement in second harmonic imaging: discriminating between muscle and collagen. Proceedings of SPIE, 2009, , .	0.8	0
43	Assessing structural characteristics of axons in cortical neurons using polarization sensitive SHG. Proceedings of SPIE, 2010, , .	0.8	0
44	Improving image quality in small animal diffusion tensor imaging at 7T. , 2012, , .		0
45	1H Spectroscopic Imaging of the Rodent Brain. Methods in Molecular Biology, 2018, 1718, 189-202.	0.9	0